

# Shot noise in NS junctions with Weyl superconductor

A. Golub

*Department of Physics, Ben-Gurion University of the Negev Beer-Sheva, Israel*

(Dated: April 22, 2019)

We demonstrate that current-current correlations (in particular the shot noise), can be used to study the intrinsic superconductivity in a slightly doped Weyl semi-metal. The systems studied is an N-WS tunneling junction where the left electrode is a normal metal while the right electrode is a Weyl superconductor (WS). The superconductivity supports surface state with crossed flat bands thereby impact the low energy spectrum. This spectrum displays a modified density of states in the gap region that strongly affects transport characteristics of the N-WS junction. The Fano factor is calculated as function of the applied bias, and shown to be dependent essentially on the orientation of the surface of WS relative to the tunneling direction. If this orientation supports the occurrence of low energy state, then the shot noise power decreases with decreasing voltage, a property similar to that prevailing in a junction with Majorana bound state.

PACS numbers: 73.43.-f, 74.45.+c, 73.23.-b, 71.10. Pm.

**Introduction:** Occurrence of new class of materials, referred to as Weyl semimetals (WSM), was predicted theoretically<sup>1-9</sup> and recently realized in experiments<sup>10-22</sup>. Below a certain critical temperature, a WSM becomes a Weyl superconductor (WS), as studied in theory<sup>23-30</sup> and in experiment<sup>31</sup>. Above the critical temperature, WSM have, in general, a finite bulk conductance and hence they can be considered as metallic. At the same time, a semi-metal phase is realized when the Fermi energy touches the Weyl point where there is a contact between the filled valence and empty conduction bands. Interestingly, the Weyl points act as monopole source in momentum space for Berry phase.

Semi-metallicity is unstable against doping that moves the Fermi level into conduction or valence bands, thereby reaching the phase of Weyl metal or even a WS. WSM host Fermi arcs and require breaking time-reversal or inversion symmetries. Weyl metals preserve the topology of Weyl nodes and topological properties of Fermi surface like Fermi arcs. These arcs are terminated by projecting Weyl points on the surface Brillouin zone. The superconductivity of doped WSMs supports crossed flat bands and not only simple arcs<sup>30</sup>.

**Objectives of this work** In this work we expose the physics of an N-WS junction between a normal metal (N) and a WS with uniform pairing state (which is essential for the occurrence of crossed flat bands). The novel aspect here, of course, is encoded in the superconducting side of the junction, that is remarkably distinct from that of a usual superconductor. Indeed, upon slight doping with finite chemical potential  $\mu$ , a WSM has disconnected Fermi surfaces, each of which surrounds a band-touching Weyl points. (Doping of WSM is easily achieved by modifying the chemical potential such that it is much larger than the gap of the WS, that is,  $\mu \gg \Delta$ .) A special form of the order parameter can be realized on these Fermi surfaces, corresponding either to BCS s-wave phase or to the Fulde-Ferrell-Larkin-Ovchinnikov (FFLO) phase. In the first case, the pairing occurs between states related by inversion symmetry (if it exists), while in the FFLO

phase the states of opposite sides of each Fermi surface are paired. A constant s-wave pairing can support bulk gap nodes on the Fermi surface<sup>23</sup> (nodal superconductor).

To elucidate the peculiar physics of the N-WS junction we write down the corresponding low energy Hamiltonian, and then calculate the shot noise power of the the junction and display it as a function of applied voltage. It is shown that depending on the orientation of the surface of the WS relative to tunneling direction the creation of novel surface states<sup>30</sup> can strongly affect the shot noise power and electron transport. Technically, our approach uses the Green's function (GF) of the WS integrated over momentum. The GF depends crucially on the boundary conditions at the N-WS surface of contact, and therefore encodes the corresponding direction of the tunneling electrons. Three cases are considered here: (1-2) N-WS junction with respective tunneling directions along the x and z axes, and 3) (for comparison), NS junction between normal metal and homogenous s-wave superconductor.

**Model:** The low energy Hamiltonian for the N-WS junction reads  $H = H_N + H_T + H_{WS}$ , where the left lead (N) is biased by voltage  $V$  and its Hamiltonian reads  $H_N = \frac{1}{2} \sum_k \epsilon_k c_{kL}^\dagger \sigma_0 \tau_z c_{kL}$ . The tunneling Hamiltonian for the point contact is  $H_T = w c_L^\dagger(0) \sigma_0 \tau_z c_R(0) + h.c.$ , where  $w$  is the junction tunneling constant. On the right side, the WS is described by two band lattice model Hamiltonian which depends on an integer parameter  $m$  that controls the number and positions of the Weyl points. Here we will use the low energy quasiclassical hamiltonian<sup>23,26,28,30</sup>

$$H_{SW} = \frac{1}{2} \sum_k c_{kR}^\dagger [v(k_x \sigma_y \tau_z - k_y \sigma_x \tau_0) - v_z k_z \sigma_z \tau_z - \mu \sigma_0 \tau_z - \Delta \sigma_y \tau_y] c_{kR} \quad (1)$$

where  $v_z = t_z \sin(Q)$ ,  $k_i = -i\partial_i$ , ( $i = x, y, z$ ). The Hamiltonian (1) encodes the low energy spectrum near the Weyl point  $(0,0,Q)$ . This spectrum plays a crucial role in the study of transport and noise processes. Denot-

ing  $c_{\mathbf{k}} = (c_{k\uparrow}, c_{-k\downarrow}, c_{-k\uparrow}^\dagger, c_{k\downarrow}^\dagger)^T$  and  $H_{SW} = \frac{1}{2} \sum_{\mathbf{k}} c_{\mathbf{k}}^\dagger \mathcal{H}_{\mathbf{k}} c_{\mathbf{k}}$ . Then  $\mathcal{H}_{\mathbf{k}}$  corresponds to a  $4 \times 4$  operator valued matrix acting in spin $\otimes$ Nambu space in which  $\sigma_i$  ( $\tau_i$ ) are the respective Pauli matrices. A useful technique to properly handle the boundary conditions at the contact is to use the hamiltonian (1) also for the N side ( $x < 0$ ) by letting  $\Delta(x < 0) = 0$  and adding to  $H_{SW}$  a term  $M\sigma_z\tau_z\theta(-x)^{30,32}$ . At the end we take the limit  $M \rightarrow \infty$ .

The current operator is defined as derivative of number of electrons in the left lead (say):

$$j = -ie[N_L, H] = -ie[\frac{w}{2}c_L^\dagger(0)\sigma_0\tau_0c_R(0) - h.c.]. \quad (2)$$

To proceed, we write down the corresponding Keldysh action to which we add a source field  $\alpha(x)$  that multiplies the current operator. Explicitly,

$$S_{ef} = \sum_{k,k'} \int dt \{ \text{Tr} [c_k^\dagger \hat{g}_{k,k'}^{-1} c_k] \}. \quad (3)$$

$$\begin{aligned} \hat{g}_{k,k'}^{-1} &= g_{k,k'}^{-1} \delta_{k,k'} - \Sigma_{T,k,k'}, \\ \Sigma_{T,k,k'} &= w A_{k,k'} \sigma_0 (\varrho_x \tau_z \rho_0 + i \varrho_y \alpha \tau_0 \rho_x). \end{aligned} \quad (4)$$

Here the subscript  $k = (\mathbf{k}L)$ ,  $(\mathbf{k}R)$  of the spinors  $c_k$  refers also to (L,R) (left,right) space described by  $\varrho$  matrices and Keldysh ( $\rho$  matrices). Moreover,  $A_{k,k'} = 1$  presents a constant matrix in momentum space  $k, k'$ . The Green functions (GF) of the leads are diagonal in LR space, that is,  $g_k^{-1} = g_{Lk}^{-1} P_{e+} + g_{Rk}^{-1} P_{e-}$  where  $P_{e\pm} = (1 \pm \varrho_z)/2$ . We denote  $g_{Lk}$  as the Keldysh GF of normal metal and  $g_{Rk}$  as GF of the superconductor in NS junction. The crucial point is that  $g_{Rk}$  depends on the direction of the tunneling electrons, which, in turns, affects the shot noise and the conductance of the N-WS junction.

Now we are in a position to write down the expressions for current and current noise following variation of the action (3) with respect to the quantum source field  $\alpha$

$$J = \frac{ie}{2} \text{Tr} [\hat{g} \frac{\partial}{\partial \alpha(t)} \hat{g}^{-1}] \quad (5)$$

$$S(t, t') = \frac{-e^2}{4} \text{Tr} [\hat{g} (\frac{\partial}{\partial \alpha(t)} \hat{g}^{-1}) \hat{g} \frac{\partial}{\partial \alpha(t')} \hat{g}^{-1}] \quad (6)$$

where trace includes also the integration over momentum and time variables. Expressions for the GF  $\hat{g}$  are obtained by calculating the inverse of block matrix  $\hat{g}^{-1}$  in LR space. After this is completed, summation over momentum in the expressions for the current and the noise can be easily carried out. The results are expressed solely in terms of GF integrated over momentum, given by,

$$\bar{G} = \begin{pmatrix} G_{LL} & G_{LR} \\ G_{RL} & G_{RR} \end{pmatrix}, \quad (7)$$

where  $G_{ii} = 2\pi N_i g_{ii}$  and  $G_{ij} = \frac{4x}{w} g_{ij}$  ( $i \neq j$ ). Here  $g_{ii} = (\bar{g}_i^{-1} - 4x\tau_z \bar{g}_j \tau_z)^{-1}$ ,  $g_{ij} = \bar{g}_i \tau_z g_{jj}$ . The effective tunneling width  $x = \pi^2 w^2 N_L N_W$  depends on the density

of states of the normal metal lead  $N_L$  as well as on the density of states of the WS  $N_W = \mu^2 / (4\pi^2 v^2 v_z)$ . Thus, the shot noise power and the stationary current in terms of these GFs acquire a form

$$J = \frac{ew}{2} \text{Tr} [i \varrho_y \rho_x] = 2ex \text{Tr} (g_{LR}^K - g_{LR}^{\bar{K}}), \quad (8)$$

$$S = -e^2 x (S_1 - 4x S_2), \quad (9)$$

$$\begin{aligned} S_1 &= 2 \text{Tr} [g_{LL} \rho_x g_{RR} \rho_x], \\ S_2 &= \text{Tr} [g_{LR} \rho_x g_{LR} \rho_x + (L \leftrightarrow R)], \end{aligned} \quad (10)$$

where the superscript  $K$  denotes the Keldysh GF. Explicit expressions for Keldysh, retarded and advanced GF, as well as for the noise and the tunneling current, are presented in the Appendix.

NS junction with S-wave superconductor: The homogeneous s-wave superconductor has no states in the gap region. The imaginary part of integrated over momentum diagonal components of  $g_R^r$  is equal to zero in the gap region. After the momentum integration  $g_R^r$  for s-wave pairing itself has a standard form (trivially enlarge to spin space the result of ref.<sup>33</sup>). We calculate shot noise and Fano factor, the tunneling current and conductance for this type of NS junction. The result as function of tunneling transparency are presented in the Fig.1-3 by right panels. The conductance there and in all other figures is given in terms of transmission coefficient :  $T_n = 4x/(1+x)^2$ .

NWS junction, tunneling along  $\hat{z}$ : Discussion

As we have already stressed, for the NWS junction, the GF is determined by boundary conditions at the contact surface, and the result strongly depends on the respective tunneling direction<sup>30</sup>. For tunneling along the  $z$  direction, an approximate expression for the GF follows directly from the Hamiltonian, in which all derivatives are considered as a moments (including the  $z$ -component). This approximation is justified for the  $z$  direction starting from the Hamiltonian (1), because the surface of the WS that is perpendicular to the  $z$ -axis does not introduce new low energy states and thus does not influence transport property of the NWS junction. However, the topology of WS results here in nodal structure of effective order parameter. To see this let us at first for notational convenience renormalize the components of the momentum for isotropic case as  $k_{x,y}/(\mu/v) \rightarrow k_{x,y}$ ,  $k_z/(\mu/v_z) \rightarrow k_z$ . This enables us to write

$g_{Rk}^r = \frac{1}{\mu} [\frac{\xi}{\mu} \sigma_0 \tau_0 - k_x \sigma_y \tau_z + k_y \sigma_x \tau_0 + k_z \sigma_z \tau_z + \sigma_0 \tau_z + \frac{\Delta}{\mu} \sigma_y \tau_y]^{-1}$ . Inverting this  $4 \times 4$  matrix involves a denominator which contains a factor  $\epsilon^2 - \xi^2 - (\Delta \sin \theta)^2$  where, in rescaled form,  $\xi = (|\vec{k}| - 1)$ . The central ingredient for evaluating conductance and noise is  $g_{Rk}^r$ , that is, the GF integrated over momentum. The denominator appearing in  $g_{Rk}^r$  (whose detailed expression is given in Appendix), clearly indicates a nodal structure of the effective order parameter.

NWS junction tunneling along  $\hat{z}$ : Results

The left panels in Figs. 1-3 display the Fano factor,

current density and conductance. The results show a remarkable similarity with those pertaining to d-wave superconductors<sup>34</sup>

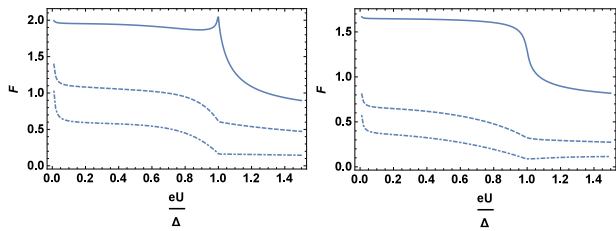


FIG. 1: Fano factor as function of applied voltage  $eU/\Delta$  for different values of tunneling width  $x$ . Solid, dashed, dot-dashed curves correspond to  $x=0.1, 0.5$  and  $0.7$ , respectively. Left panel presents NS junction with Weyl nodal superconductor, right one stands for NS contact where  $S$  is a standard gapped s-wave superconductor.

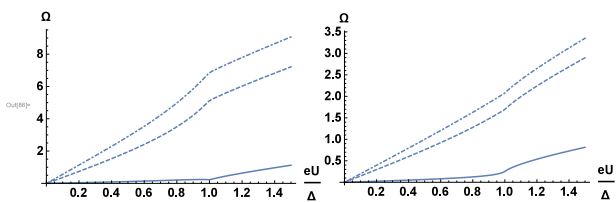


FIG. 2: The same NS junctions as in Fig.1. The plot represents the current  $\Omega = J/e$  -voltage dependence.

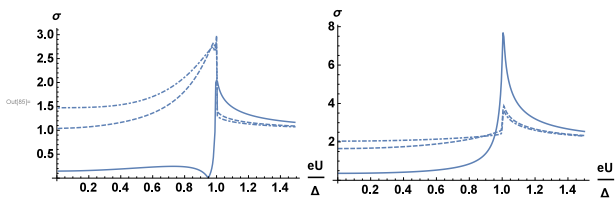


FIG. 3: The conductance  $\sigma$  (normalized by normal conductance) as function of applied voltage with the same sets of parameters and the same NS junctions ( as in Fig1 and Fig2 ) is considered.

#### NWS junction, tunneling along $\hat{x}$ : Discussion

The GF of the WS satisfies boundary conditions on a surface perpendicular to the  $x$ -axis (at  $x=0$ ). This is the basic element required for the derivation of the shot noise and electron transport along  $\hat{x}$ , where the topological nature of the WS is clearly exposed<sup>30</sup>. The behavior of the conductance and the shot noise is determined by the structure of the flat band and the nature of the low energy states that occur for  $\epsilon \ll \Delta$ . We must obtain Green function  $g_R^r$  to find the spectrum and calculate the shot noise power. The expression for the corresponding GF (detailed derivation is given in Appendix) reads

$$g_R^r = g_d \hat{I} - g_{off} \tau_y \sigma_y \quad (11)$$

where  $g_d$  and  $g_{off}$  integrated over momentum components of  $g_R^r$ . NWS junction, tunneling along  $\hat{x}$ : Results The imaginary part  $g_R^r$  (diagonal components) displays a

peak of the density of states in the middle of superconductive gap region (Fig.4, left panel).

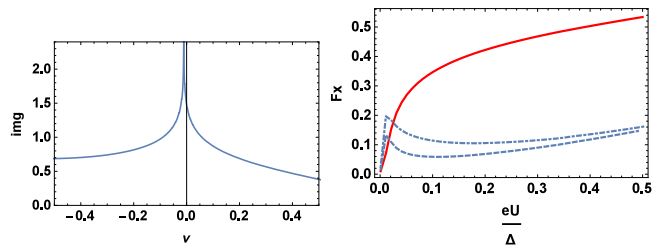


FIG. 4: Left panel: Density of states of Weyl superconductor with a surface orthogonal to  $x$ -axis versus energy in the gap region. A peak of the density in the gap region is the effect related to topological reconstruction of the spectra. The right panel presents Fano factor as function of applied voltage. The same sets of parameters as in Fig1-3 for tunneling in  $x$ -direction were used: The lines correspond to  $x=0.1$  (red solid),  $0.5$  (dashed),  $0.7$  (dot-dashed).

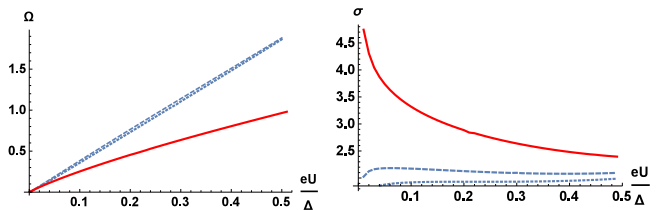


FIG. 5: The I-V characteristics of NWS junction for tunneling in  $x$  direction (left panel) and conductance in  $x$ -direction ( $\sigma$ ) as function of voltage(right panel). The same sets of parameters as in Fig.4 (right panel) was used.

The right panel of Fig.4 presents the Fano factor, for the the NWS junction (with tunneling along the  $x$ - direction), while the tunneling current and the conductance for this case are respectively displayed on the left and right panels of Fig.5. At the smallest value of transmission parameter  $x = 0.1$  there is a peak of conductance at  $V \rightarrow 0$  which is similar to the zero bias conductance peak obtained in<sup>30</sup> for nonzero control parameter  $m$ . The quite different as compared with other cases (Fig.1-3) voltage dependence of Fano factor. This difference originates from the occurrence of the peak in the density of states at zero energy which exists only when WS (described by hamiltonian (1)) has a boundary plane perpendicular to  $x$ -axes.

Our main result As far as the shot noise, Fano factor and conductances are concerned, comparing our results for tunneling along  $z$  with those of tunneling along  $x$  we note a remarkable feature. The shot noise power at low voltage is rather small. Such behavior of the shot noise is similar to that encountered for tunneling in a junction with Majorana bound state<sup>35-38</sup>. Indeed, the formula for the total shot noise in this case<sup>35</sup> is given by equation

$$S = \frac{8e^2\Gamma}{h} \left( \arctan \frac{eV}{2\Gamma} - \frac{2eV\Gamma}{(eV)^2 + 4\Gamma^2} \right) \quad (12)$$

where  $\Gamma$  is the tunneling width. Thus we see that as the

bias voltage  $V \rightarrow 0$  both the noise power and its first derivative vanish:  $(\frac{dS}{dV})_{V=0} = 0$ . i. e. the transport is coherent. Moreover, it is found that the conductance has zero bias peak as shown in Fig. 5 (here it takes place for small tunneling strength  $x=0.1$ ). This result is based on the analyzes of the approximate quasiclassical hamiltonian (1) without using the parameter  $m$  from the exact tight-binding model<sup>23,30</sup>. Nevertheless, the singularities in the spectrum (like peak at zero energy) are preserved and influence the conductance for small  $x$ .

*Conclusions:* In this work we suggest that measurements of shot noise serve as an additional benchmark for studying the topological properties of Weyl superconductors. The superconductivity itself can support surface crossed flat bands. The specific topology of WSM is presented by point nodes in the s-wave pairing state<sup>30</sup>. For the model described by the hamiltonian (1), different tunneling directions are not equivalent: for  $z$  direction tunneling, the boundary does not create in-gap states, while for conductance along the  $x$  axis flat band structure of low energy spectrum causes the final density of states in the middle of the gap that strongly influences the transport and the shot noise power. In particular, the shot noise has similarity with tunneling via Majorana bound states (instead of WS) at least for decreasing  $S$  at  $V \rightarrow 0$ .

In closing we remark on the approximations that were made here. First, the parameter  $m$  which controls the positions of the Weyl points is not employed in our calculations while it was considered in the complete tight-binding model<sup>30</sup>. However, based on the approximate quasiclassical hamiltonian (1), the nontrivial topology related to the surface of WS orthogonal to the  $x$ -axis clearly reveals itself via zero bias peak in the conductance and in the shot noise power (that decreases at small voltage). Why there is such a difference it is not clear. It may be related to the fact that the relevant low energy spectrum of WS originates from hamiltonian (1).

Second, we used an approach that describes the electron tunneling in the same way as for a point junction. The right electrode is a superconductor which is characterized by its GFs properly integrated over momenta. However, while for a  $z$ -directed transport the inhomogeneity along the  $z$ -axis is irrelevant and may be ignored in deriving the shot noise, for  $x$ -tunneling direction the inhomogeneity along the  $x$ -axis (due to the superconductor's surface) is relevant. In the latter case we solved the boundary value problem and found an approximate expression for the GF restricted to flat band spectrum and, therefore it is related to the boundary conditions at the surface. The corresponding spectrum then defines the low energy physics which is responsible for tunneling in NS junctions.

## Appendix A

### 1. Shot noise in NS junctions with Weyl superconductor

Here we provide the derivation of the shot noise power for NS junctions with different tunneling directions and present the total list of Green's functions which were used.

The noise formula in the main text (Eqs 9,10) after taking the trace in Keldysh space acquires a form

$$\begin{aligned} S_1 &= 2tr\{4Im[g_{LL}^r]Im[g_{RR}^r] + g_{RR}^K g_{LL}^K\} \\ S_2 &= tr\{4Im[g_{LR}^r]Im[g_{LR}^r] + g_{LR}^K g_{LR}^K + (L \leftrightarrow R)\} \end{aligned} \quad (A1)$$

The trace also includes integration over energy variable ( $\nu$ ). The GFs which are involved in above expression for noise have a form:

(a) left (N) electrode GF without tunneling interaction (we have dropped here and below the bar at  $g$ )

$$\begin{aligned} g_L^K &= -i(\tanh \frac{\nu - eV}{2T} P_+ + \tanh \frac{\nu + eV}{2T} P_-) \\ g_L^{r,a} &= \mp \frac{i}{2} \hat{I}, \quad P_{\pm} = \frac{1}{2}(\hat{I} \pm \tau_z \sigma_0) \end{aligned}$$

where  $\hat{I}$  is unit matrix in four dimensional case.

(b) The integrated over momentum non-interacting GF of superconductor  $g_R$  as explained in the main text depends on tunneling direction. The Keldysh component of this GF is simply  $g_R^K = \tanh[\frac{\nu}{2T}](g_R^r - g_R^a)$ .

The left and right electrode GFs are modified by tunneling

$$g_{LL}^{r,a} = \mp \frac{i}{2} (\hat{I} \pm 2ix\tau_z \sigma_0 g_{RR}^{r,a} \tau_z \sigma_0)^{-1} \quad (A2)$$

$$g_{RR}^{r,a} = (g_R^{r,a-1} \pm 2ix)^{-1} \quad (A3)$$

and for Keldysh GFs we have

$$\begin{aligned} g_{LL}^K &= \tanh \frac{\nu}{2T} (g_{LL}^r - g_{LL}^a) + 4A_L \\ g_{RR}^K &= \tanh \frac{\nu}{2T} (g_{RR}^r - g_{RR}^a) + 4xA_R \end{aligned}$$

where we used notation

$$A_i = g_{ii}^r \hat{F} g_{ii}^a, \quad \hat{F} = g_L^K + i\hat{I} \tanh \frac{\nu}{2T} \quad (A4)$$

and  $i = L, R$ .

The crossed GFs appear due to tunneling processes. They can be written in terms of modified by tunneling diagonal GFs of each electrode

$$\begin{aligned} g_{LR}^{r,a} &= \mp \frac{i}{2} \tau_z \sigma_0 g_{RR}^{r,a} \\ g_{RL}^{r,a} &= g_R^{r,a} \tau_z \sigma_0 g_{LL}^{r,a} \end{aligned} \quad (A5)$$

The crossed Keldysh GFs acquire a form

$$\begin{aligned} g_{LR}^K &= \tanh \frac{\nu}{2T} (g_{LR}^r - g_{LR}^a) + \tau_z \sigma_0 g_R^{r-1} A_R \\ g_{RL}^K &= \tanh \frac{\nu}{2T} (g_{RL}^r - g_{RL}^a) + 4g_R^r \tau_z \sigma_0 A_L \end{aligned} \quad (\text{A6})$$

Using these formulas the current and the noise power can be transformed to

$$\begin{aligned} J &= 2e \text{tr} \{ \hat{F} [g_{RR}^a \tau_z \sigma_0 g_R^{r-1} g_{RR}^r - 4g_{LL}^a g_R^r \tau_z \sigma_0 g_{LL}^r] \} \\ S_1 &= 8 \text{tr} \{ \tanh \frac{\nu}{2T} [(g_{RR}^r - g_{RR}^a) A_L + x A_R (g_{LL}^r - g_{LL}^a)] + \\ &\quad 4x A_R A_L \} + S_{1N} \end{aligned} \quad (\text{A7})$$

and to a more complicated expression for  $S_2$

$$\begin{aligned} S_2 &= 4x \text{tr} \{ \tau_z \sigma_0 g_R^{r-1} A_R \tau_z \sigma_0 g_R^{r-1} A_R + \\ &\quad 16g_R^r \tau_z \sigma_0 A_L g_R^r \tau_z \sigma_0 A_L + \\ &\quad \tanh \frac{\nu}{2T} [2(g_{LR}^r - g_{LR}^a) \tau_z \sigma_0 g_R^{r-1} A_R + \\ &\quad 8(g_{RL}^r - g_{RL}^a) g_R^r \tau_z \sigma_0 A_L] \} + S_{2N} \end{aligned} \quad (\text{A8})$$

Here  $S_{1N}$ ,  $S_{2N}$  present the Naikwist part of the noise power, and are given, respectively, by the fist terms in  $S_1$ ,  $S_2$  (Eq.A1) with a factor  $(1 - (\tanh \frac{\nu}{2T})^2)$ .

## 2. Integrated Green's Functions

The 3D momentum integration of  $g_{Rk}^r$  for z-tunneling direction consists of integrations on  $\xi$  and on polar angles  $(\theta, \varphi)$

$$\begin{aligned} g_R^r &= h_1 \Theta[1 - \nu^2] + h_2 \Theta[-1 + \nu^2] \\ h_1 &= x_1 \nu \hat{I} - x_2 \tau_y \sigma_y \\ h_2 &= y_1 |\nu| \hat{I} - y_2 \text{sign}[\nu] \tau_y \sigma_y \end{aligned}$$

here  $\nu = \epsilon/\Delta$  and

$$\begin{aligned} x_1 &= \frac{1}{4} (\pi - 2i \text{arcsinh}[\frac{\nu}{\sqrt{1-\nu^2}}] \text{sign}[\nu]) \\ x_2 &= \frac{1}{8\nu} (\pi \nu (1 + \nu^2) + 2i |\nu| (v - \\ &\quad (1 + \nu^2) \arcsin(\frac{\nu}{\sqrt{1-\nu^2}})) \\ y_1 &= -\frac{i}{4} \ln[(1 + |\nu|)/(-1 + |\nu|)] \\ y_2 &= \frac{1}{8} i (2|\nu| + (1 + \nu^2) \ln[1 - 2/(1 + |\nu|)]) \end{aligned}$$

It is more difficult, though standard, to obtain the integrated over momentum GF of a superconductor with surface plane perpendicular to x axis. Looking for eigenvalues of  $\det[g_{R,k}^{-1}] = 0$  we find 4 eigenvalues  $\pm p, \pm p^*$  and

corresponding four eigenvectors  $w_1, w_2, w_3, w_4$

$$\begin{aligned} w_1 &= \exp(-ipx) \{ \gamma^* \tan \frac{\theta}{2}, -i\gamma^* \exp(-i\varphi), \\ &\quad i \exp(-i\varphi) \tan \frac{\theta}{2}, 1 \} \\ w_2 &= \exp(ipx) \{ \gamma^* \tan \frac{\theta}{2}, i\gamma^* \exp(i\varphi), \\ &\quad -i \exp(i\varphi) \tan \frac{\theta}{2}, 1 \} \\ w_3 &= \exp(-ip^*x) \{ \gamma \tan \frac{\theta}{2}, -i\gamma \exp(-i\varphi), \\ &\quad i \exp(-i\varphi) \tan \frac{\theta}{2}, 1 \} \\ w_4 &= \exp(ip^*x) \{ \gamma \tan \frac{\theta}{2}, i\gamma \exp(i\varphi), -i \exp(i\varphi) \tan \frac{\theta}{2}, 1 \} \end{aligned} \quad (\text{A9})$$

here  $k_y = \sin \theta \cos \varphi$ ,  $k_z = \cos \theta$ ,  $\gamma = \sqrt{\frac{\nu-i\zeta}{\nu+i\zeta}}$ ; and  $\zeta = \sqrt{\sin^2 \theta - \nu^2}$ . For eigenvalue  $p$  we get

$$p = \sqrt{1 - k_x^2 - k_y^2 - 2i\zeta} \quad (\text{A10})$$

The eigenvalues and their eigenvectors can be obtained also for left (normal metal) electrode. However, to calculate the GF of superconductor only two eigenvectors of normal metal are sufficient. After taking the limit  $M \rightarrow \infty$  at  $x = 0$  these vectors acquire a form:  $u_1 = \{0, 0 - 1, 1\}$ ,  $u_2 = \{-1, 1, 0, 0\}$ .

The retarded GF of superconductor satisfies equation  $(\nu - H_{SWk})g_R^r(x, x') = \delta(x - x')$  where  $H_{SWk}$  is given by expression in square brackets of Eq.(1) (main text) with rescaled values of momentums. The GF can be expressed in terms of eigen vectors as

$$\begin{aligned} g_R^r(x, x') &= \Theta(x - x') [b_1(x') w_1(x) + b_2(x') w_4(x)] + \\ &\quad \Theta(x' - x) [a_1(x') w_1(x) + a_2(x') w_2(x) + \\ &\quad a_3(x') w_3(x) + a_4(x') w_4(x)] \end{aligned} \quad (\text{A11})$$

where we have took in consideration the convergence of GF at  $x \rightarrow \infty$ . To find functions  $a_i(x)$  and  $b_j(x)$  we use boundary conditions at  $x = 0$  and at  $x = x'$ . Two terms  $a_i$  ( $i=2,3$ ) are completely defined by conditions at  $x = x'$ . They are not related with boundary at  $x = 0$ . Therefore, these terms do not contribute in relevant low energy physics and we neglect them in GF. After integration over  $\varphi$  the matrix GF of Weyl superconductor acquires a simple form with only two different coefficients:

$$g_R^r(\theta) = G_d \hat{I} - G_{off} \tau_y \sigma_y \quad (\text{A12})$$

Here

$$G_d(x=0, \theta) = -\frac{\pi \sin^2 \theta d_0 \tan[\frac{\theta}{2}]}{\sqrt{\cos^2 \theta + \nu^2}} \quad (\text{A13})$$

$$G_{off}(x=0, \theta) = -\frac{\pi \nu \sin \theta d_0}{\sqrt{\cos^2 \theta + \nu^2}} \quad (\text{A14})$$

were  $\sin \theta$  from  $d^3p$  differential has been included in Eqs.(A13, A14). Factor  $d_0$  reads

$$d_0 = i \left[ \frac{\Theta(\sin \theta - |\nu|)}{\sqrt{\sin^2 \theta - \nu^2}} - \frac{2 \operatorname{sign}(\nu) \Theta(-\sin \theta + |\nu|)}{\pi \sqrt{-\sin^2 \theta + \nu^2}} \ln(\sqrt{-1 + \beta_-^2} + |\beta_-|) \right] - \frac{2 \operatorname{sign}(\nu) \Theta(\sin \theta - |\nu|)}{\pi \sqrt{\sin^2 \theta - \nu^2}} \ln(\sqrt{1 + \beta_+^2} - |\beta_+|)$$

were  $\beta_{\pm} = \nu / [\sqrt{\pm(\sin^2 \theta - \nu^2)} \cos \theta]$ ,

The GF  $g_R^r$  in the main text (Eq.(11)) ready follows after integration over  $\theta$  variable:  $g_d = \int_0^\pi d\theta G_d$  and  $g_{off} = \int_0^\pi d\theta G_{off}$ .

### Acknowledgments

I would like to thank B. Horovitz, Y. Avishai and E. Grossfeld for stimulating discussions and for valuable remarks.

- 
- <sup>1</sup> X. Wan, A. M. Turner, A. Vishwanath, and S. Y. Savrasov, Phys. Rev. B 83, 205101 (2011).
- <sup>2</sup> K.-Y. Yang, Y.-M. Lu, and Y. Ran, Phys. Rev. B 84, 075129 (2011).
- <sup>3</sup> A. A. Burkov and L. Balents, Phys. Rev. Lett. 107, 127205 (2011).
- <sup>4</sup> G. Xu, H. Weng, Z. Wang, X. Dai, and Z. Fang, Phys. Rev. Lett. 107, 186806 (2011).
- <sup>5</sup> S. M. Young, S. Zaheer, J. C. Y. Teo, C. L. Kane, E. J. Mele, and A. M. Rappe, Phys. Rev. Lett. 108, 140405 (2012).
- <sup>6</sup> Z. Wang, Y. Sun, X.-Q. Chen, C. Franchini, G. Xu, H. Weng, X. Dai, and Z. Fang, Phys. Rev. B 85, 195320 (2012).
- <sup>7</sup> Z. Wang, H. Weng, Q. Wu, X. Dai, and Z. Fang, Phys. Rev. B 88, 125427 (2013).
- <sup>8</sup> H. Weng, C. Fang, Z. Fang, B. A. Bernevig, and X. Dai, Phys. Rev. X 5, 011029 (2015).
- <sup>9</sup> S.-M. Huang, S.-Y. Xu, I. Belopolski, C.-C. Lee, G. Chang, B. Wang, N. Alidoust, G. Bian, M. Neupane, C. Zhang, S. Jia, A. Bansil, H. Lin, and M. Z. Hasan, Nat Commun 6 (2015).
- <sup>10</sup> S.-Y. Xu, I. Belopolski, N. Alidoust, M. Neupane, C. Zhang, R. Sankar, S.-M. Huang, C.-C. Lee, G. Chang, B. Wang, G. Bian, H. Zheng, D. S. Sanchez, F. Chou, H. Lin, S. Jia, and M. Zahid Hasan, ArXiv e-prints (2015), arXiv:1502.03807 [cond-mat.mes-hall].
- <sup>11</sup> B. Q. Lv, H. M. Weng, B. B. Fu, X. P. Wang, H. Miao, J. Ma, P. Richard, X. C. Huang, L. X. Zhao, G. F. Chen, Z. Fang, X. Dai, T. Qian, and H. Ding, ArXiv e-prints (2015), arXiv:1502.04684 [cond-mat.mtrl-sci].
- <sup>12</sup> S.-Y. Xu, C. Liu, S. K. Kushwaha, R. Sankar, J. W. Krizan, I. Belopolski, M. Neupane, G. Bian, N. Alidoust, T.-R. Chang, H.-T. Jeng, C.-Y. Huang, W.-F. Tsai, H. Lin, P. P. Shibayev, F.-C. Chou, R. J. Cava, and M. Zahid Hasan, ArXiv e-prints (2015), arXiv:1501.01249 [cond-mat.meshall].
- <sup>13</sup> L. Lu, Z. Wang, D. Ye, L. Ran, L. Fu, J. D. Joannopoulos, and M. Soljačić, ArXiv e-prints (2015), arXiv:1502.03438 [cond-mat.mtrl-sci].
- <sup>14</sup> C. Zhang, S.-Y. Xu, I. Belopolski, Z. Yuan, Z. Lin, B. D. S. Sanchez, H. Zheng, G. Bian, J. Wang, C. Zhang, T. Neupert, M. Zahid Hasan, and S. Jia, ArXiv e-prints (2015), arXiv:1503.02630 [cond-mat.mes-hall].
- <sup>15</sup> B. Q. Lv, N. Xu, H. M. Weng, J. Z. Ma, P. Richard, X. C. Huang, L. X. Zhao, G. F. Chen, C. Matt, F. Bisti, V. Strokov, J. Mesot, Z. Fang, X. Dai, T. Qian, M. Shi, and H. Ding, ArXiv e-prints (2015), arXiv:1503.09188 [cond-mat.mtrl-sci].
- R. Chang, H. Zheng, V. Strokov, D. S. Sanchez, G. Chang, Z. Yuan, D. Mou, Y. Wu, L. Huang, C.-C. Lee, S.-M. Huang, B. Wang, A. Bansil, H.-T. Jeng, T. Neupert, A. Kaminski, H. Lin, S. Jia, and M. Zahid Hasan, ArXiv e-prints (2015), arXiv:1504.01350 [cond-mat.mes-hall].
- <sup>16</sup> S. Borisenko, Q. Gibson, D. Evtushinsky, V. Zabolotnyy, B. Büchner, and R. J. Cava, Phys. Rev. Lett. 113, 027603 (2014).
- <sup>17</sup> Z. K. Liu, B. Zhou, Y. Zhang, Z. J. Wang, H. M. Weng, D. Prabhakaran, S.-K. Mo, Z. X. Shen, Z. Fang, X. Dai, Z. Hussain, and Y. L. Chen, Science 343, 864 (2014).
- <sup>18</sup> M. Neupane, S.-Y. Xu, R. Sankar, N. Alidoust, G. Bian, C. Liu, I. Belopolski, T.-R. Chang, H.-T. Jeng, H. Lin, A. Bansil, F. Chou, and M. Z. Hasan, Nat. Commun. 5 (2014).
- <sup>19</sup> S.-Y. Xu, N. Alidoust, I. Belopolski, C. Zhang, G. Bian, T.-R. Chang, H. Zheng, V. Strokov, D. S. Sanchez, G. Chang, Z. Yuan, D. Mou, Y. Wu, L. Huang, C.-C. Lee, S.-M. Huang, B. Wang, A. Bansil, H.-T. Jeng, T. Neupert, A. Kaminski, H. Lin, S. Jia, and M. Zahid Hasan, ArXiv e-prints (2015), arXiv:1504.01350 [cond-mat.mes-hall].
- <sup>20</sup> T. Sato, K. Segawa, K. Kosaka, S. Souma, K. Nakayama, K. Eto, T. Minami, Y. Ando, and T. Takahashi, Nat Phys 7, 840 (2011).
- <sup>21</sup> Q. Li, D. E. Kharzeev, C. Zhang, Y. Huang, I. Pletikoscic, A. V. Fedorov, R. D. Zhong, J. A. Schneeloch, G. D. Gu, and T. Valla, ArXiv e-prints (2014), arXiv:1412.6543 [cond-mat.str-el].
- <sup>22</sup> R. Y. Chen, S. J. Zhang, J. A. Schneeloch, C. Zhang, Q. Li, G. D. Gu, and N. L. Wang, ArXiv e-prints (2015), arXiv:1505.00307 [cond-mat.mtrl-sci].
- <sup>23</sup> G. Y. Cho, J. H. Bardarson, Y.-M. Lu, and J. E. Moore, Phys. Rev. B 86, 214514 (2012).
- <sup>24</sup> V. Shivamoggi and M. J. Gilbert, Phys. Rev. B 88, 134504 (2013).
- <sup>25</sup> H. Wei, S.-P. Chao, and V. Aji, Phys. Rev. B 89, 235109 (2014).
- <sup>26</sup> H. Wei, S.-P. Chao, and V. Aji, Phys. Rev. B 89, 014506 (2014).
- <sup>27</sup> G. Rednik, A. A. Zyuzin, and A. A. Burkov, arXiv:1506.05109 [cond-mat].
- <sup>28</sup> T. Meng and L. Balents, Phys. Rev. B 86, 054504 (2012).
- <sup>29</sup> M. H. Fischer, T. Neupert, C. Platt, A. P. Schnyder, W. Hanke, J. Goryo, R. Thomale, and M. Sgrist, Phys. Rev.

- B 89, 020509 (2014).
- <sup>30</sup> B. Lu, K. Yada, M. Sato, and Y. Tanaka, Phys. Rev. Lett. 114, 096804 (2015).
- <sup>31</sup> F. C. Chen, X. Luo, R. C. Xiao, W.J. Lu, B. Zhang, H.X. Yang, J. Q. Li, Q. L. Pei, D. F. Shao, R. R. Zhang, L. S. Ling, C. Y. Xi, W. H. Song, Y. P. Sun, arXiv:1512.08175
- <sup>32</sup> A. C. Potter, I. Kimchi and A. Vishwanath, Nature Communications 5:5161 — DOI: 10.1038/ncomms6161
- <sup>33</sup> G. B. Arnold, journal of Low Temp. Phys. 68, 1, (1987)
- <sup>34</sup> S. Kashiwaya and Y. Tanaka. Rep. Prog. Phys. 63, 1641, (2000)
- <sup>35</sup> A. Golub and B. Horovitz, Phys. Rev. B 83, 153415 (2011).
- <sup>36</sup> A. Haim, E. Berg, F.von Oppen, and Y. Oreg, Phys. Rev. B 92, 245112 (2015).
- <sup>37</sup> S. Valentini, M. Governale, R. Fazio, and F. Taddei, Physica E 75, 15 (2016).
- <sup>38</sup> K. M. Tripathi, S. Das, and S. Rao, arXiv:1509.06684 .